



Optimal generation scheduling of interconnected wind-coal intensive power systems

Wang, S., Yu, D., Yu, J., Zhang, W., Foley, A., & Li, K. (2016). Optimal generation scheduling of interconnected wind-coal intensive power systems. IET Generation, Transmission and Distribution. DOI: 10.1049/iet-gtd.2016.0086

Published in:

IET Generation, Transmission and Distribution

Document Version:

Peer reviewed version

Queen's University Belfast - Research Portal:

[Link to publication record in Queen's University Belfast Research Portal](#)

Publisher rights

Copyright 2016 IET.

This paper is a postprint of a paper submitted to and accepted for publication in IET Generation, Transmission and Distribution and is subject to Institution of Engineering and Technology Copyright. The copy of record is available at IET Digital Library.

General rights

Copyright for the publications made accessible via the Queen's University Belfast Research Portal is retained by the author(s) and / or other copyright owners and it is a condition of accessing these publications that users recognise and abide by the legal requirements associated with these rights.

Take down policy

The Research Portal is Queen's institutional repository that provides access to Queen's research output. Every effort has been made to ensure that content in the Research Portal does not infringe any person's rights, or applicable UK laws. If you discover content in the Research Portal that you believe breaches copyright or violates any law, please contact openaccess@qub.ac.uk.

Optimal Generation Scheduling of Interconnected Wind-Coal Intensive Power Systems

Songyan Wang^{1,2}, Daren Yu¹, Jilai Yu², Wei Zhang², Aoife Foley³, Kang Li⁴,

1. *Postdoctoral Research Station of Power Engineering and Engineering
Thermalphysics, Harbin Institute of Technology, Harbin, China*

2. *School of Electrical Engineering and Automation, Harbin Institute of Technology,
Harbin, China*

3. *School of Mechanical and Aerospace Engineering, Queen's University Belfast,
United Kingdom*

4. *School of Electronics, Electrical Engineering and Computer Science, Queen's
University Belfast, United Kingdom*

* *Corresponding author. Tel.: +44-(0)7462729260; fax: +44-(0)2890975449.*

E-mail address: wangsongyan@163.com (Songyan Wang)

Abstract

Large scale wind power generation complicated with restrictions on the tie line plans may lead to significant wind power curtailment and deep cycling of coal units during the valley load periods. This paper proposes a dispatch strategy for interconnected wind-coal intensive power systems. Wind power curtailment and cycling of coal units are included in the economic dispatch analysis of regional systems. Based on the day-ahead dispatch results, a tie line power plan adjustment strategy is implemented in the event of wind power curtailment or deep cycling occurring in the economic dispatch model, with the objective of reducing such effects. The dispatch strategy is designed based on the distinctive operation characteristics of interconnected wind-coal intensive power systems, and dispatch results for regional systems in China show that the proposed strategy is feasible and can improve the overall system operation performance.

30 *Key word:* wind power, interconnections, generation scheduling, coal cycling,
31 wind-coal intensive system

32 **Nomenclature**

33 *Acronyms*

34 SE sending end system

35 RE receiving end system

36 ASE power adjustment model of the SE

37 ARE power adjustment model of the RE

38 EPAC excessive power accommodation capability

39 UC unit commitment

40 WCIS wind-coal intensive power system

41 IWCIS interconnected system with WCIS and load center

42 *Sets*

43 Ω_{br} set of branch lines in RE

44 Ω_{bs} set of branch lines in SE

45 Ω_{dps} set of deep cycling units in SE

46 Ω_{gr} Set of normal units in RE

47 Ω_{gs} Set of normal units in the SE

48 Ω_{ws} Set of wind farms in the SE

49 *SE modelling*

50 *Objective functions*

51 C_{com} total operation cost in SE

52 C_{cur} cost of the wind power curtailment in SE

53 C_{dyc} deep cycling cost of the deep cycling units in SE

54 C_{dnom} normal status cost of the deep cycling units in SE

55	C_{gnom}	operation cost of normal units in SE
56	C_{res}	spinning reserve cost in SE
57	C_{tot}	total operation cost of deep cycling unit
58	$f_{\text{dnom},j}$	normal status cost function of the deep cycling unit j
59	$f_{\text{gnom},i}$	operation cost function of the normal unit i
60	<i>Parameters</i>	
61	D_{dp}	number of average deep cycling days of deep cycling unit per year
62	E_{cur}	maximum allowed curtailed wind energy
63	$E_{\text{dp}}^{(av)}$	average deep cycling energy per day of deep cycling unit
64	L_t	predicted load at time t
65	P_i^{max}	maximum power of normal unit or deep cycling unit
66	P_i^{min}	minimum power of normal unit
67	P_j^{nommin}	minimum power of deep cycling unit j in normal operation area
68	P_j^{dpmin}	minimum power of deep cycling unit j in deep cycling area
69	$P_{\text{tie},t}^{\text{plan}}$	original tie line plan at time t
70	$R_i^{\text{up,max}}$	maximum upward reserve of normal unit i
71	$R_i^{\text{up,min}}$	minimum upward reserve of normal unit i
72	$R_i^{\text{dn,max}}$	maximum downward reserve of normal unit i
73	$R_i^{\text{dn,min}}$	minimum downward reserve of normal unit i
74	$R_{\text{sysup},t}$	upward reserve demand of the system at time t
75	$R_{\text{sysdn},t}$	downward reserve demand of the system at time t
76	$R_{\text{wup},t}$	upward reserve demand of the wind power at time t
77	$R_{\text{wdn},t}$	downward reserve demand of the wind power at time t

78	S_{dp}	generation capacity of deep cycling unit
79	T	number of dispatch intervals
80	ΔT	time interval
81	\overline{T}_k	capacity of line k
82	$W_{form,t}$	predicted wind power of wind power plant n at time t
83	$\underline{W}_{errn,t}$	lower bound of the prediction interval of the n^{th} wind power plant
84	$\overline{W}_{errn,t}$	upper bound of the prediction interval of the n^{th} wind power plant
85	b_{om}	annual operation & maintenance cost per unit of deep cycling unit
86	c_{dpj}	unit cost of deep cycling unit j in deep cycling area
87	c_{wn}	unit cost of the wind power curtailment of wind farm n
88	$k_{i,t}^{\text{up}}$	unit cost of upward spinning reserve of normal unit i at time t
89	$k_{i,t}^{\text{dn}}$	unit cost of downward spinning reserve of normal unit i at time t
90	$r_{i,\text{up}}$	upward regulation rate of unit i
91	$r_{i,\text{dn}}$	downward regulation rate of unit i
92	ρ	lifespan reduction factor of deep cycling unit
93	<i>Variables</i>	
94	$P_{i,t}$	generation scheduling of normal unit i at time t
95	$P_{k,t}$	power of line k at time t
96	$R_{i,t}^{\text{up}}$	upward reserve of normal unit i at time t
97	$R_{i,t}^{\text{dn}}$	downward reserve of normal unit i at time t
98	$W_{schen,t}$	scheduled wind power output of the wind power plant n at time t
99	$\delta P_{j,t}^{(d)}$	magnitude between P_j^{nomin} and P_j^{dpmin} at time t
100	$\delta P_{j,t}^{(n)}$	magnitude between P_j^{max} and P_j^{nomin} at time t

101 ***RE modelling***

102 *Parameters*

103 $\Delta P_{\text{EPAC},t}^{\text{RE}}$ excessive power accommodation capability of the RE at time t

104 $P_{i,t}^{\text{RE}}$ optimized power output of normal unit i from RE modelling

105 k_h parameter of the slight adjustment

106 ***ASE modelling***

107 *Objective functions*

108 ΔC_{ASE} adjusted total cost of the SE

109 ΔC_{cur} adjusted cost of the wind power curtailment of the SE

110 ΔC_{gnom} adjusted cost of normal units in SE

111 ΔC_{dnom} adjusted normal status cost of the deep cycling units in SE

112 ΔC_{dcyc} adjusted deep cycling cost of the deep cycling units in SE

113 ΔC_{tie} adjusted cost for the tie line plan adjustment

114 *Parameters*

115 P_{TTC} total transfer capability of tie line

116 $P_{i,t}^{\text{SE}}$ optimized power output of normal unit i from SE modelling

117 $P_{k,t}^{\text{SE}}$ power of line k at time t from SE modelling

118 $W_{\text{schen},t}^{\text{SE}}$ scheduled wind power output of the wind power plant n at time t from SE

119 modelling

120 c_{tie} unit cost of tie line power adjustment

121 $c_{\text{dnom},j}$ unit cost of deep cycling unit j in normal area

122 $c_{\text{gnom},i}$ unit cost of power adjustment of normal unit i

123 t_{start} the time interval when wind power curtailment first occurs in dispatch results

124 of SE modelling

- 125 t_{end} the time interval when wind power curtailment last occurs
- 126 $\delta P_{j,t}^{\text{SE}(d)}$ optimized $\delta P_{j,t}^{(d)}$ of normal unit i from SE modelling
- 127 $\delta P_{j,t}^{\text{SE}(n)}$ optimized $\delta P_{j,t}^{(n)}$ of deep cycling unit j from SE modelling
- 128 λ_{ik} branch flow sensitivity with respect to normal unit i
- 129 λ_{jk} branch flow sensitivity with respect to deep cycling unit j
- 130 λ_{nk} branch flow sensitivity with respect to wind farm n
- 131 *Variables*
- 132 $\Delta P_{i,t}$ adjusted generation scheduling of normal unit i at time t
- 133 $\Delta P_{j,t}^{(d)}$ adjusted magnitude between P_j^{nomin} and P_j^{dpmn} at time t
- 134 $\Delta P_{j,t}^{(n)}$ adjusted magnitude between $P_j^{\text{max}(n)}$ and P_j^{nomin} at time t
- 135 $\Delta W_{\text{schen},t}$ adjusted scheduled wind power output of the wind power plant n at time t
- 136 $\Delta P_{\text{tie},t}$ adjusted tie line plan
- 137 *ARE modelling*
- 138 *Objective functions*
- 139 ΔC_{ARE} adjusted total cost of the RE
- 140 *Parameters*
- 141 $\Delta P_{\text{tie},t}^{\text{ASE}}$ optimized tie line power adjustment from ASE modelling
- 142 *Other Parameters*
- 143 $C_a^{(D)}$ accumulated cost of wind power curtailment and deep cycling within D days
- 144 $C_{\text{as}}^{(D)}$ accumulated cost of wind power curtailment, deep cycling and start-up of
- 145 coal units within D days
- 146 $C_{\text{cur}}^{(d)}$ cost of the wind power curtailment in d^{th} day
- 147 $C_{\text{dcyc}}^{(d)}$ deep cycling cost in d^{th} day

148 C_s start-up cost of coal units

149 D number of operation days

150

151

152

153 **1 Introduction**

154 **1.1 Motivation and aims**

155 Emission-free power generation and sustainable energy supply are two key
156 benefits of the wind power. With the increase of wind power penetration [1], the
157 anti-correlation between wind power and system demand increases the operation
158 pressure of the system [2, 3]. For systems with high wind penetration, evidences show
159 that the operation flexibility is sensitive to wind power fluctuations during the valley
160 load periods for systems with coal-fired units as the dominant generators (e.g.
161 Colorado in the USA, Germany, Poland and China) [4-6]. As wind power generation
162 may be very high during the valley load period, in order to maintain the power
163 balance, power output of coal units in these systems may experience “deep cycling”
164 [4]. In deep cycling status, the power level of coal units is below their normal
165 minimum bound, and the operation cost is very high due to increased plant
166 maintenance and reduced plant lifespan.

167 Long start-up time, high start-up cost and high minimum power output are key
168 features of coal fired units. Unlike short start-up time of gas turbine units, the cold
169 start-up time of coal units is around 20 hours or even longer. Meanwhile, the
170 minimum shut-down time of coal units also takes several hours, which further extends
171 the out-of-service state of coal units [7, 8]. Besides, coal units in these systems often
172 have very large capacities and they cannot be shut down flexibly. Further, the start-up

173 costs of coal units are extremely high and significantly affect the overall operational
174 costs of the system. Such features force coal units to be scheduled in a 72-hour
175 residual unit commitment (UC) or weekly UC [9, 10]. That is to say, UC of coal units
176 can be seen as fixed for day ahead scheduling. Hence, power systems with coal-fired
177 units as major generators lack the capability to cope with large wind power variance,
178 and such systems are also described as Wind-Coal Intensive Systems (WCIS).

179 Generally speaking, WCIS are always connected with other load centers by long
180 distance transmission lines [11] as most wind farms are often far away from the load
181 centers. Such interconnected power systems have some distinctive characteristics as
182 the sending end system is the WCIS and the receiving end system is a load center, and
183 these multi-area systems are named as interconnected WCIS (IWCIS) which exist in
184 the USA, China and other countries [6, 12]. Similar to conventional interconnected
185 systems that can procure reserve assistance from neighboring areas [13], WCIS can
186 also acquire assistance from the load center for accommodating excessive wind power.
187 However, as the original tie line plans are often implemented through contracts that
188 are strictly followed by regional systems [14], the coordination of WCIS may
189 experience severe inflexibility along with the rapid increase of wind power
190 generations.

191 This paper primarily aims to establish an optimal dispatch model of WCIS which
192 considers both the wind power curtailment and deep cycling of coal units. Based on
193 the optimized dispatch results of each regional system, the tie line plan adjustment
194 strategy of IWCIS is proposed. The tie line power adjustment strategy aims at
195 relieving deep cycling and wind curtailment of WCIS by exploiting surplus generation
196 capacity from the load center.

197 1.2 Literature review and contributions

198 Various issues regarding wind power accommodation and multi-area system
199 coordination can be found in many existing publications. For wind power
200 accommodation, Wang *et al.* [5] demonstrated that coal units cannot provide a
201 favorable environment for accommodating variable wind generation. Albadi [15]
202 concluded that higher integration costs can be incurred due to the intermittent nature
203 of the wind power. Chang *et al.* [16] proposed a new optimal power flow algorithm
204 and revealed that wind generation systems will affect the bus voltage and transmission
205 losses. Chun [17] proved that wind power curtailment may reduce system operation
206 cost significantly. Doherty *et al.* [18] studied the impact of wind power on the system
207 operation cost and the carbon emissions of the Irish system dominated by gas
208 generation. For multi-area system operation, Khatir *et al.* [13] proposed an augmented
209 Lagrangian algorithm to optimally schedule the generating units of multi-area systems.
210 Ying *et al.* [14] proposed an approach to incorporate contracts into multi-area UC
211 solutions, and coal units were treated as “must-run” generators due to their long
212 start-up time. Chung *et al.* [19] utilized Benders decomposition to deal with multi-area
213 unit commitment problems. Soroudi and Rabiee [20] proposed a multi-area dynamic
214 economic dispatch model, taking into account wind power generation and power pool
215 market to supply the overall demand of the system for a given horizon. Abdullah *et al.*
216 [21] developed a wind resource sharing strategy for an interconnected system to
217 achieve the national and regional renewable energy target.

218 Although the impact of wind power on the regional system operation has been
219 intensively researched, distinctive operation features of WCIS are barely discussed in
220 the literature. These features include:

221 (i) The UC of WCIS can be seen as fixed as the start-up cost of coal units is usually
222 high while the start-up time of coal units is very long.

223 (ii) Wind power curtailment and deep cycling of coal units are very likely to occur.

224 (iii) Unit cost of deep cycling is extremely higher than other unit operation costs.

225 The operation feature (i) indicates that 0/1 binary variables for describing the
226 start-up/shut-down statuses of coal units in conventional UC models can be avoided in
227 the optimal scheduling of WCIS. For operation feature (ii), as the deep cycling status
228 and the normal operational status of coal units are different, this operation feature may
229 lead to a mixed integer problem. Operation feature (iii) indicates that reducing deep
230 cycling should be in a primary aim in the day-ahead dispatch model of WCIS.

231 Ideally, the grid operator could centrally regulate all the interconnected systems.
232 However, in reality, due to various political, economical and technical reasons, such
233 operations are rarely implemented for multi-area systems as the operational
234 independence is a distinctive feature of the interconnected systems [13]. Generally, a
235 tie line power plan of a multi-area system is often made based on the obligation
236 contracts and is strictly implemented by regional systems during the whole system
237 operation. Thus, it is rather difficult to achieve the global optimality of the operation
238 cost of interconnected power systems [22].

239 In this paper, the economic dispatch model and tie line plan adjustment strategy
240 are proposed, which take into account of the distinctive operation characteristics of
241 IWCIS, distinctively from existing approaches. We propose a deep cycling model that
242 can avoid the 0/1 problems in economic dispatch. Further, we propose two measures
243 for the tie line power adjustment during valley load periods, namely the timing
244 window and excessive power accommodation capability (EPAC) of the load center,
245 which both help IWCIS to accommodate large penetration of wind power.

246 The remaining paper is organized as follows. Section 2 discusses the operation
247 characteristics of WCIS and the decompositions of IWCIS. Section 3 details the

248 WCIS modelling, and proposes the new tie line plan adjustment strategy. Section 4
249 presents case studies of a typical IWCIS to confirm the efficacy of the proposed
250 strategy. Conclusions and discussions are given in Section 5.

251 **2 Mechanism of tie line power adjustment of IWCIS**

252 **2.1 Operation characteristics of WCIS during valley load periods**

253 Wind power plants are often given high priority in generating power, and the
254 price of wind power is legally allowed to be higher than normal price of electricity
255 generated by coal units [23]. For coal units, the unit cost of deep cycling is usually
256 much higher than that of wind power. In this paper, all unit costs are based on the
257 current electric price policy of China [5]. Deep cycling is a very special operational
258 status for coal units, it is only applied to maintain the power balance, and coal units in
259 deep cycling status do not participate in offering spinning reserve during valley load
260 periods. It should also be noted that not all coal units take part in deep cycling
261 regulation.

262 The anti-correlation between wind power and load during off-peak periods is
263 illustrated in Fig. 1. The load and wind power data used in this paper is extracted from
264 a typical WCIS in Northern China. Generation equipment and power output statistics
265 of the WCIS are shown in Table 1.

266 In Fig. 1, during the valley load period, the minimum net load of the WCIS is
267 around 4600 MW. Neglecting the effect of energy storage systems, the normal
268 minimum power output of coal units is 840 MW higher than the minimum net load.
269 To maintain the power balance, wind power curtailment is required first until the
270 generated wind power reaches the maximum limit, then deep cycling of coal units is
271 adopted later to ride through the valley load period. It is clear that the coal units will
272 be forced to operate in a more stressed-out deep cycling mode after the nuclear units

273 are put into operation.

274 From the optimization point of view, as the cost of deep cycling of coal units is
275 extremely higher than other operation costs of generation units, deep cycling would be
276 the last measure for the system to keep the power balance, and reducing the deep
277 cycling cost should be given a high priority in minimizing the operation cost of WCIS
278 during optimization. As wind power curtailment and deep cycling have significant
279 impact on the operation cost of WCIS, it is obvious that the time periods for both
280 wind power curtailment and deep cycling are the key time durations that WCIS can
281 procure assistance from the connected load center.

282 **2.2 Decomposition of IWCIS**

283 A simplified topology of IWCIS is shown in Fig. 2. Based on Fig. 2, the
284 generation scheduling of IWCIS can be formulated as the following steps:

285 (1) As the original tie line power plans are made based on the energy contracts and
286 can be seen as a constant in a relatively long time interval, the sending end system and
287 receiving end system can be treated as two isolated regional power systems, thus the
288 model of the sending end system (SE) and the model of the receiving end system (RE)
289 can be established independently.

290 (2) Based on the optimized result of the SE model, the wind power curtailment and
291 deep cycling power of coal units in the SE model can be obtained. Meanwhile, the
292 excessive power accommodation capability (EPAC) of the RE can also be calculated
293 from the RE model.

294 (3) Based on the time duration of the wind power curtailment or deep cycling in the
295 SE model, the timing window for the tie line power adjustment of WCIS can then be
296 calculated, and the power adjustment of the tie line can only be implemented in this
297 timing window.

298 (4) During the timing window for the tie line power adjustment, the power adjustment
299 model of the SE (ASE) can be established. The objective of this model is to reduce
300 both the wind power curtailment and the deep cycling of the units in the SE.
301 Meanwhile, the obtained power adjustment of the tie line in ASE model is also
302 restricted by EPAC of the RE. The adjusted power of the tie line reflects the reduction
303 of the wind power curtailment and deep cycling.

304 (5) Once the tie line power adjustment is obtained from the ASE model, the optimal
305 power adjustment model for the RE (ARE) can be established. The objective of the
306 ARE model is to minimize the adjusted operation cost of the RE with the adjusted tie
307 line power.

308 The flow chart of the strategy is shown in Fig. 3, where two decompositions are
309 applied in the modelling process, namely the decomposition of SE and RE, and the
310 decomposition of ASE and ARE. The first decomposition is based on the operation
311 independence and contract obligation between two regional systems. The second
312 decomposition follows two steps, the first step is to achieve EPAC of the RE, and the
313 second step is to send the tie line adjustment information from SE back to the RE .
314 The information interchange in this process is concise which fully considers the
315 operation independence of regional systems.

316 **3 Modelling of IWCIS**

317 **3.1 Deep Cycling Modelling**

318 The power output characteristics of coal units with deep cycling capability are
319 shown in Fig. 4.

320 As shown in Fig. 4, once the power output of the coal units is lower than P^{nomin} ,
321 the coal units will be operated in the deep cycling status.

322 The unit cost of the deep cycling unit c_{dp} is set as follows:

$$c_{dp} = \frac{b_{om} S_{dp} \rho}{E_{dp}^{(av)} D_{dp}} \quad (1)$$

Parameters in (1) can be obtained from retired coal units that were involved in deep cycling. c_{dp} is extremely high due to the lifespan reduction of deep cycling generators, which is reflected by ρ .

In Fig. 4, P^{nomin} can be seen as a bound to distinguish the normal operation status from the deep cycling status. To avoid solving a mixed integer problem in deep cycling modelling, two continuous variables $\delta P^{(d)}$ and $\delta P^{(n)}$ which fully exploit the significant difference between c_{dp} and c_{gnom} are defined in the deep cycling modelling, as shown in Fig. 4. It should be noted that $\delta P^{(d)}$ and $\delta P^{(n)}$ are not variables to represent the actual power outputs of the coal units, but instead they are variables to describe the magnitude differences between power limits of coal units. From Fig. 4, the power limits of $\delta P^{(n)}$ and $\delta P^{(d)}$ are:

$$\begin{cases} 0 \leq \delta P^{(n)} \leq P^{\max} - P^{nomin} \\ 0 \leq \delta P^{(d)} \leq P^{nomin} - P^{dpmin} \end{cases} \quad (2)$$

The total operation cost of the deep cycling unit C_{tot} is:

$$\begin{aligned} C_{tot} &= C_{dnom} + C_{dcyc} \\ \begin{cases} C_{dnom} = f_{dnom}(P^{nomin} + \delta P^{(n)}) \\ C_{dcyc} = c_{dp}(P^{nomin} - P^{dpmin} - \delta P^{(d)}) \end{cases} \end{aligned} \quad (3)$$

In (3), the deep cycling level of the coal power plant is denoted by the difference between P^{nomin} and $P^{dpmin} + \delta P^{(d)}$. Bigger difference implies severer deep cycling operation.

Assume the objective of the SE model is set to minimize the operation cost of the SE. As c_{dp} is much higher than the costs of other generation units, avoiding deep cycling is the primary target in the objective optimization. If wind power output is not high and the dispatch situation during the valley load period is not severe, the

345 optimized result for $\delta P^{(d)}$ will be $P^{\text{nomin}} - P^{\text{dpmin}}$ and $\delta P^{(n)}$ will be greater than zero. On
 346 the contrary, if the wind power is high and deep cycling units tend to operate in the
 347 deep cycling mode during the valley load period, $\delta P^{(n)}$ will be reduced to 0 first due to
 348 the power balance constraint. Then $P^{\text{dpmin}} + \delta P^{(d)}$ will become smaller than P^{nomin} to
 349 maintain the power balance. Consequently, no matter a deep cycling unit is in normal
 350 status or in deep cycling status, the power output can both be expressed as:

$$351 \quad P = P^{\text{dpmin}} + \delta P^{(d)} + \delta P^{(n)} \quad (4)$$

352 According to (4), P includes $\delta P^{(d)}$ and $\delta P^{(n)}$ and both variables are continuous,
 353 thus P can be optimized throughout while meeting all physical constraints in the
 354 WCIS modelling, and the mixed integer optimization problem is thus avoided.

355 3.2 Spinning reserve modelling of wind power

356 Empirical distribution function can be adopted to approximate the probability
 357 distribution of wind power prediction error. It is assumed that the future wind power
 358 prediction errors follow the same error probability distribution of historic prediction
 359 errors [24]. After the extreme forecasting errors are eliminated, the largest negative
 360 and positive prediction errors (e.g., values beyond 6 times of the standard deviation of
 361 the forecasting error) of the n^{th} wind power plant are denoted as [5]

$$362 \quad \left\{ (\underline{W}_{\text{errn},t}, \overline{W}_{\text{errn},t}), t = 1, 2, \dots, T \right\} \quad (5)$$

363 The spinning reserve demand of the total wind power in SE can be then obtained
 364 by:

$$365 \quad \begin{cases} R_{\text{wup},t} = \sum_{n \in \Omega_{\text{ws}}} \underline{W}_{\text{errn},t} \\ R_{\text{wdn},t} = \sum_{n \in \Omega_{\text{ws}}} \overline{W}_{\text{errn},t} \end{cases} \quad (6)$$

366 3.3 SE modelling and timing window for tie line power adjustment

367 The objective is given as follows:

368

$$\min C_{\text{com}} = C_{\text{gnom}} + C_{\text{dnom}} + C_{\text{deyc}} + C_{\text{res}} + C_{\text{cur}} \quad (7)$$

$$369 \quad \begin{cases} C_{\text{gnom}} = \sum_{t=1}^T \sum_{i \in \Omega_{\text{gs}}} f_{\text{gnom},i}(P_{i,t}) \\ C_{\text{dnom}} = \sum_{t=1}^T \sum_{j \in \Omega_{\text{dps}}} f_{\text{dnom},j}(P_j^{\text{nomin}} + \delta P_{j,t}^{(n)}) \\ C_{\text{res}} = \sum_{t=1}^T \sum_{i \in \Omega_{\text{gs}}} (k_{i,t}^{\text{up}} R_{i,t}^{\text{up}} + k_{i,t}^{\text{dn}} R_{i,t}^{\text{dn}}) \\ C_{\text{deyc}} = \sum_{t=1}^T \sum_{j \in \Omega_{\text{dps}}} c_{\text{dpj}} (P_j^{\text{nomin}} - P_j^{\text{dpmin}} - \delta P_{j,t}^{(d)}) \\ C_{\text{cur}} = \sum_{t=1}^T \sum_{n \in \Omega_{\text{ws}}} c_{\text{wn}} (W_{\text{form},t} - W_{\text{schen},t}) \end{cases}$$

370 s.t.

$$371 \quad \sum_{i \in \Omega_{\text{gs}}} P_{i,t} + \sum_{n \in \Omega_{\text{ws}}} W_{\text{schen},t} + \sum_{j \in \Omega_{\text{dps}}} (P_j^{\text{dpmin}} + \delta P_{j,t}^{(d)} + \delta P_{j,t}^{(n)}) = L_t + P_{\text{tie},t}^{\text{plan}} \quad (8)$$

$$372 \quad \sum_{t=1}^T \sum_{n \in \Omega_{\text{ws}}} (W_{\text{form},t} - W_{\text{schen},t}) \Delta T \leq E_{\text{cur}} \quad n \in \Omega_{\text{ws}} \quad (9)$$

$$373 \quad W_{\text{schen},t} \leq W_{\text{form},t} \quad n \in \Omega_{\text{ws}} \quad (10)$$

$$374 \quad P_i^{\text{min}} \leq P_{i,t} \leq P_i^{\text{max}} \quad i \in \Omega_{\text{gs}} \quad (11)$$

$$375 \quad 0 \leq \delta P_{j,t}^{(d)} \leq P_j^{\text{nomin}} - P_j^{\text{dpmin}} \quad j \in \Omega_{\text{dps}} \quad (12)$$

$$376 \quad 0 \leq \delta P_{j,t}^{(n)} \leq P_j^{\text{max}} - P_j^{\text{nomin}} \quad j \in \Omega_{\text{dps}} \quad (13)$$

$$377 \quad -r_{i,\text{dn}} \Delta T \leq P_{i,t} - P_{i,t-1} \leq r_{i,\text{up}} \Delta T \quad i \in \Omega_{\text{gs}} \quad (14)$$

$$378 \quad -r_{j,\text{dn}} \Delta T \leq (P_j^{\text{dpmin}} + \delta P_{j,t}^{(d)} + \delta P_{j,t}^{(n)}) - (P_j^{\text{dpmin}} + \delta P_{j,t-1}^{(d)} + \delta P_{j,t-1}^{(n)}) \leq r_{j,\text{up}} \Delta T \quad j \in \Omega_{\text{dps}} \quad (15)$$

$$379 \quad |P_{k,t}| \leq \bar{T}_k, \quad k \in \Omega_{\text{bs}} \quad (16)$$

$$380 \quad \begin{cases} \sum_i R_{i,t}^{\text{up}} \geq R_{\text{sysup},t} + R_{\text{wup},t} \\ P_{i,t} + R_{i,t}^{\text{up}} \leq P_i^{\text{max}} \\ R_i^{\text{up},\text{min}} \leq R_{i,t}^{\text{up}} \leq R_i^{\text{up},\text{max}} \end{cases} \quad i \in \Omega_{\text{gs}} \quad (17)$$

$$381 \quad \begin{cases} \sum_i R_{i,t}^{\text{dn}} \geq R_{\text{sysdn},t} + R_{\text{wdn},t} \\ P_{i,t} - R_{i,t}^{\text{dn}} \geq P_i^{\text{min}} \\ R_i^{\text{dn},\text{min}} \leq R_{i,t}^{\text{dn}} \leq R_i^{\text{dn},\text{max}} \end{cases} \quad i \in \Omega_{\text{gs}} \quad (18)$$

382

The objective in (7) minimizes the operation cost of normal coal units, deep

383 cycling units, spinning reserve procurement and wind power curtailment. Equation (8)
384 is the power balance constraint for WCIS. Equations (9) and (10) are the constraints
385 for the maximum wind power curtailment and the maximum scheduled wind power,
386 respectively. Equations (11-13) are the power output bounds of normal coal units and
387 deep cycling units, respectively. Equations (14) and (15) model the ramping
388 constraints of normal units and deep cycling units, respectively. Equation (16) models
389 the maximum limits of branch line flows. Equations (17) and (18) model the
390 constraints of upward and downward spinning reserves, respectively.

391 By solving the SE model, the optimized dispatch results for $P_{i,t}^{SE}$, $W_{schen,t}^{SE}$,
392 $\delta P_{j,t}^{SE(d)}$ and $\delta P_{j,t}^{SE(n)}$ can be achieved. According to the SE modelling analysis in
393 Section 3.1, if $\delta P_{j,t}^{SE(n)} > 0$, then $\delta P_{j,t}^{SE(d)} = P_j^{nomin} - P_j^{dpmin}$. Under this circumstance, the
394 corresponding coal unit is operated in the normal operational region. However, if
395 $\delta P_{j,t}^{SE(n)} = 0$, then $\delta P_{j,t}^{SE(d)} \leq P_j^{nomin} - P_j^{dpmin}$, which implies deep cycling occurs in the
396 SE model.

397 Suppose that the first time interval when wind power curtailment occurs
398 according to the dispatching results of the SE model is denoted as t_{start} , and the time
399 interval when the last wind power curtailment occurs is denoted as t_{end} , then the
400 timing window for the tie line power adjustment can be set as $[t_{start}, t_{end}]$.

401 3.4 RE modelling and calculation of EPAC

402 The RE modelling has the same procedure as the SE modelling, but the deep
403 cycling and wind power curtailment are both neglected in the RE modelling due to
404 high load level in the load center. Based on the optimized results of RE, the EPAC of
405 the RE ($\Delta P_{EPAC,t}^{RE}$) is given as:

$$406 \quad \Delta P_{EPAC,t}^{RE} = \sum_{i \in \Omega_{gr}} \min(P_{i,t}^{RE} - P_i^{min}, k_h r_{i,dn} \Delta T) \quad (19)$$

407 The EPAC reflects downward generation space in the load center. Generally, load
 408 centers with larger generation capacity have a stronger EPAC to accommodate wind
 409 power from the WCIS.

410 3.5 ASE Modelling

411 Within the whole time intervals $[t_{\text{start}}, t_{\text{end}}]$, the ASE modelling is formulated as
 412 the following maximization problem,

$$413 \quad \max \quad \Delta C_{\text{ASE}} = \Delta C_{\text{cur}} + \Delta C_{\text{dcyc}} - \Delta C_{\text{gnom}} - \Delta C_{\text{dnom}} - \Delta C_{\text{tie}} \quad (20)$$

$$414 \quad \begin{cases} \Delta C_{\text{cur}} = \sum_{t=t_{\text{start}}}^{t_{\text{end}}} \sum_{n \in \Omega_{\text{ws}}} c_{\text{wn}} \Delta W_{\text{schen},t} \\ \Delta C_{\text{dcyc}} = \sum_{t=t_{\text{start}}}^{t_{\text{end}}} \sum_{j \in \Omega_{\text{dps}}} c_{\text{dpj}} \Delta P_{j,t}^{(d)} \\ \Delta C_{\text{gnom}} = \sum_{t=t_{\text{start}}}^{t_{\text{end}}} \sum_{i \in \Omega_{\text{gs}}} c_{\text{gnomi}} \Delta P_{i,t} \\ \Delta C_{\text{dnom}} = \sum_{t=t_{\text{start}}}^{t_{\text{end}}} \sum_{j \in \Omega_{\text{dps}}} c_{\text{dnomj}} \Delta P_{j,t}^{(n)} \\ \Delta C_{\text{tie}} = \sum_{t=t_{\text{start}}}^{t_{\text{end}}} c_{\text{tie}} \Delta P_{\text{tie},t} \end{cases}$$

415 s.t.

$$416 \quad \sum_{i \in \Omega_{\text{gs}}} \Delta P_{i,t} + \sum_{i \in \Omega_{\text{dps}}} (\Delta P_{j,t}^{(d)} + \Delta P_{j,t}^{(n)}) + \sum_{n \in \Omega_{\text{ws}}} \Delta W_{\text{schen},t} - \Delta P_{\text{tie},t} = 0 \quad (21)$$

$$417 \quad 0 \leq \Delta P_{i,t} \leq \min(P_i^{\text{max}} - P_{i,t}^{\text{SE}}, k_h r_{i,\text{up}} \Delta T) \quad i \in \Omega_{\text{gs}} \quad (22)$$

$$418 \quad 0 \leq \Delta P_{j,t}^{(d)} \leq \min(P_j^{\text{nomin}} - P_j^{\text{dpmi}} - \delta P_{j,t}^{\text{SE}(d)}, k_h r_{j,\text{up}} \Delta T) \quad j \in \Omega_{\text{dps}} \quad (23)$$

$$419 \quad 0 \leq \Delta P_{j,t}^{(n)} \leq \min(P_j^{\text{max}} - P_j^{\text{nomin}} - \delta P_{j,t}^{\text{SE}(n)}, k_h r_{j,\text{up}} \Delta T) \quad j \in \Omega_{\text{dps}} \quad (24)$$

$$420 \quad 0 \leq \Delta W_{\text{schen},t} \leq W_{\text{form},t} - W_{\text{schen},t}^{\text{SE}} \quad (25)$$

$$421 \quad \begin{aligned} \sum_{i \in \Omega_{\text{gs}}} \lambda_{ik} \Delta P_{i,t} + \sum_{j \in \Omega_{\text{dps}}} \lambda_{jk} (\Delta P_{j,t}^{(d)} + \Delta P_{j,t}^{(n)}) + \sum_{n \in \Omega_{\text{ws}}} \lambda_{nk} \Delta W_{\text{schen},t} \\ \leq \bar{T}_k - P_{k,t}^{\text{SE}}, k \in \Omega_{\text{bs}} \end{aligned} \quad (26)$$

$$422 \quad 0 \leq \Delta P_{\text{tie},t} \leq \min\{P_{\text{TTC}} - P_{\text{tie},t}^{\text{plan}}, \Delta P_{\text{EPAC},t}^{\text{RE}}\} \quad (27)$$

423 The objective in (20) maximizes the cost reduction. Note that
 424 $c_{\text{dpj}} \gg c_{\text{wn}} > c_{\text{tie}} > \max\{c_{\text{gnomi}}, c_{\text{dnomj}}\}$ and that ΔC_{tie} is the cost for the tie line plan

425 adjustment, which reflects the operation independence of interconnected power
 426 systems. Equation (21) is the constraint of the adjusted power balance. Equations (22)
 427 to (24) are the constraints of the adjusted power of normal units and the deep cycling
 428 units, respectively. $P_{i,t}^{\text{SE}}$, $\delta P_{j,t}^{\text{SE}(d)}$ and $\delta P_{j,t}^{\text{SE}(n)}$ in these equations, are all obtained
 429 from the SE modelling. Equation (25) is the constraint of wind power adjustment.
 430 Equation (26) models the branch line overloading. Equation (27) is the limits of the tie
 431 line power adjustment.

432 In (20), the objective of the ASE modelling is to reduce the wind power
 433 curtailment and deep cycling in WCIS by adjusting the tie line plan, while the
 434 adjustment of the tie line plan incurs a cost. In Equations (23) and (24), if
 435 $\delta P_{j,t}^{\text{SE}(d)} = P_j^{\text{nomin}} - P_j^{\text{dpmin}}$ in the SE modelling, then $\Delta P_{j,t}^{(d)} = 0$. If
 436 $\delta P_{j,t}^{\text{SE}(d)} \leq P_j^{\text{nomin}} - P_j^{\text{dpmin}}$, then $\Delta P_{j,t}^{(d)}$ is the optimized result which implies that the
 437 deep cycling of coal units in WCIS is reduced after the tie line plan adjustment.

438 The optimized result $\Delta P_{\text{tie},t} (\Delta P_{\text{tie},t}^{\text{ASE}})$ in the ASE modelling will be sent back to the
 439 load center for ARE modelling.

440 3.6 ARE Modelling

441 The objective of the ARE model is:

$$442 \quad \min \quad \Delta C_{\text{ARE}} = \sum_{t=t_{\text{start}}}^{t_{\text{end}}} \sum_{i \in \Omega_{\text{gr}}} c_{\text{gnomi}i} (-\Delta P_{i,t}) \quad (28)$$

443 s.t.

$$444 \quad \sum_i \Delta P_{i,t} = -\Delta P_{\text{tie},t}^{\text{ASE}} \quad i \in \Omega_{\text{gr}} \quad (29)$$

$$445 \quad \max(P_i^{\text{min}} - P_{i,t}^{\text{RE}}, -k_h r_i \Delta T) \leq \Delta P_{i,t} \leq 0 \quad i \in \Omega_{\text{gr}} \quad (30)$$

446 In (30), $P_{i,t}^{\text{RE}}$ and $\Delta P_{\text{tie},t}^{\text{ASE}}$ are obtained from the RE modelling and ASE
 447 modelling, respectively.

448 3.7 System performance indices

449 Under certain operational circumstances, shutting down a few coal units may
450 mitigate the wind power curtailment and deep cycling of coal units during the valley
451 load period. However, this is based on paying extremely high shut-down cost of coal
452 units [7]. To evaluate the benefit of shutting down coal units in WCIS, the following
453 system indices related to the long-term operation cost are adopted for system
454 performance analysis.

455 1) *Accumulated cost of wind power curtailment and deep cycling of coal units*

$$456 C_a^{(D)} = \sum_{d=1}^D \{C_{\text{cur}}^{(d)} + C_{\text{dcyc}}^{(d)}\} \quad (31)$$

457 2) *Accumulated cost of wind power curtailment, deep cycling and start-up of coal*
458 *units*

$$459 C_{\text{as}}^{(D)} = C_s + \sum_{d=1}^D \{C_{\text{cur}}^{(d)} + C_{\text{deyc}}^{(d)}\} \quad (32)$$

460 If $C_{\text{as}}^{(D)} < C_a^{(D)}$, then shutting down coal units would be more beneficial in the
461 long term than maintaining these units in operation.

462 4 Case study

463 4.1 System parameters

464 The modified Dongbei system (DB) is a WCIS [25] with 9 normal coal units, 2
465 deep cycling coal units and 3 wind farm clusters. To focus on the interactions between
466 wind power and coal units in the DB system, the energy storage system in [25] is
467 replaced by a coal unit. While the Huabei system (HB) is a simplified load center with
468 23 coal units. Both DB and HB are connected by a 500 kV transmission line, forming
469 a typical IWCIS. The installed generation capacities of DB are shown in Table 2. The
470 wind power penetration level in DB is 13.2%, which is rather high for a WCIS. The
471 original day ahead tie line plan is shown in Table 3. The dispatch interval is 15

472 minutes. Parameters for the coal units and wind farm clusters in the DB system are
473 shown in Table 4. Parameters for the coal units in HB are similar to those in DB due
474 to the same generation type. The simplified geographical layout of the DB and HB is
475 shown in Fig. 5. The predicted load and wind power curve for the DB (from intervals
476 1 to 48) are shown in Fig. 6. The allowed maximum curtailed wind energy E_{cur} for a
477 single day for DB is 800 MWh. The unit cost of the curtailed wind power (c_w) and
478 deep cycling (c_{dp}) are 1.1×10^2 \$/MWh and 2.3×10^2 \$/MWh, respectively. The spinning
479 reserve demand of the system ($R_{sysup,t}$, $R_{sysdn,t}$) and that of wind power ($R_{wup,t}$, $R_{wdn,t}$) in
480 DB are 170 MW and 50 MW in each dispatch interval, respectively.

481 4.2 Day ahead dispatch result of system DB and HB

482 The economic dispatch of DB and HB are calculated by the SE and RE models,
483 respectively. The dispatch result for DB during the valley load period is shown in
484 Table 5. It is noted that the curtailed wind power from the wind farm rather than the
485 scheduled power is shown in Table 5. To demonstrate the deep cycling level, $\delta P^{(d)}$ and
486 $\delta P^{(n)}$ of G10 and G11 are also shown.

487 According to the dispatched results, both wind power curtailment and deep
488 cycling occur within the time intervals from 7 to 24. During these intervals, G2, G3
489 and G9 all work at the minimum power output, while G1, and G4 to G8 work above
490 the minimum level to satisfy the downward reserve demand. In Table 5, the total
491 curtailed wind power is 800 MWh which already reaches its maximum limit. Both
492 wind power curtailment and deep cycling of unit G10 occur at the same time. Besides,
493 $\delta P^{(d)}$ of G10 are all smaller than 260 MW and $\delta P^{(n)}$ of G10 are all 0 MW during the
494 time intervals from 7 to 24 (i.e. power output of G10 is lower than 860 MW).
495 Meanwhile, $\delta P^{(d)}$ of G11 is 200 MW and $\delta P^{(n)}$ is 0 MW (i.e. power output of unit G11
496 is 900 MW). These results substantiate the discussions in Section 3.1. Accordingly,

497 deep cycling occurs for unit G10 during the time intervals between 7 and 24, and G11
498 maintains the critical normal operation status during these intervals, resulting in 232
499 MWh deep cycling. During the time intervals from 7 to 24, the total operation cost of
500 wind power curtailment and deep cycling is 1.41×10^5 \$. Though deep cycling energy
501 is only 0.29 times of the curtailed wind energy, the operation cost of the deep cycling
502 is 0.6 times of the wind power curtailment.

503 From Table 5, it can be seen that the time intervals from 7 to 24 with wind power
504 curtailment and deep cycling is a specific time for all generation units in DB. Then the
505 timing window for the tie line plan adjustment is also set for the time intervals from 7
506 to 24. To illustrate the relationship between wind power curtailment and deep cycling
507 during these intervals, deep cycling power of G10 and curtailment of the wind farms
508 in DB during intervals 7 to 24 are shown in Fig. 7.

509 In Fig. 7, the deep cycling curve of the G10 has strong correlation with the wind
510 power curtailment. At the beginning of the valley load period, as the load level
511 decreases, the deep cycling and wind power curtailment keep increasing. At interval
512 17, both the deep cycling power and curtailed wind power reach the maximum value
513 because the net load of DB reaches its minimum level. Later with the recovery of the
514 valley load, both deep cycling power and curtailed wind power keep decreasing and
515 finally return to 0.

516 Comparatively, due to the high load level characteristics of the load center, wind
517 power curtailment and deep cycling barely exist in HB. Thus, the dispatch pressure of
518 HB is much less than DB, and HB has the capability to accept excessive power from
519 DB. The EPAC of HB in the timing window is also shown in Table 5. It can be seen
520 that the EPAC of HB varies at different time intervals. The reason is that the total
521 power level of generation units has a strong correlation with the load variation.

522 During the valley load period the power output level of HB is also low because of its
523 low load level, which introduces small $\Delta P_{EPAC,t}$ and reduces the capability of HB to
524 accept excessive power from DB.

525 4.3 Tie line plan adjustment analysis

526 Once both SE and RE models are optimized, the power adjustment of coal units
527 and wind power plants in DB can be achieved by optimizing the ASE model. Here, c_{tie}
528 is set to 0.65×10^2 \$/MWh in this case, which is higher than the cost of normal coal
529 units in DB.

530 Results show that $\Delta P_{i,t}$ and $\Delta P_{j,t}^{(n)}$ are all 0 in the ASE modelling, which means
531 that the tie line power adjustment is mainly utilized for the recovery of deep cycling
532 power and wind power curtailment of DB. The reason is that the unit cost of tie line
533 power adjustment c_{tie} is higher than c_{gnomi} and c_{dnomj} , which blocks normal power
534 adjustment of coal units in normal operational region. In fact, $\Delta P_{i,t}$ and $\Delta P_{j,t}^{(n)}$ have
535 nonzero values only when the branch line congestion exists in the ASE model.
536 Optimized adjustment of the tie line power is shown in Fig. 8, and recovery of deep
537 cycling power and curtailed wind power in system DB is shown in Fig. 9.

538 From Fig. 8 and Fig. 9, compared with wind power curtailment, deep cycling
539 power in DB is recovered in priority due to its extremely high cost. The adjusted
540 power of G10 is equal to its deep cycling power in the SE model, which means that
541 the deep cycling power of G10 is totally recovered after the tie line power adjustment.
542 Meanwhile, during intervals 7 to 11 and intervals 22 to 24, the curtailed wind power
543 in DB is totally recovered. However, during the intervals 12 to 21, wind power
544 curtailment still exists due to the low level of EPAC of HB and the recovery priority
545 of deep cycling power.

546 After the adjustment of the tie line plan, the deep cycling energy of G10 in DB is

547 reduced to 0 and the total curtailed wind energy in DB is reduced to 366 MWh. The
548 operation cost of DB is significantly reduced by 1.01×10^5 \$, including 0.53×10^5 \$ of
549 deep cycling recovery of G10 and 0.48×10^5 \$ of curtailed wind power recovery of
550 wind farms. Meanwhile, the operational cost of HB is increased by 0.33×10^5 \$ due to
551 the power adjustment cost of coal units in HB.

552 **4.4 Influence of wind power variance to the system operation during the valley** 553 **load period**

554 Suppose the wind power fluctuation is severe, which incurs an increase of the
555 spinning reserve requirement, this will result in an increase of $R_{\text{wdn},t}$ in DB by 20 MW
556 at each dispatch interval.

557 Result shows that the power output of G1 is increased from 970 MW to 990 MW,
558 providing more downward reserves to satisfy the spinning reserve demand of the wind
559 power. Deep cycling power of G10 and total curtailed wind power in DB during
560 interval 7 to 24 are shown in Fig. 10.

561 From Fig. 10, as the power output of G1 is increased by 20 MW, to maintain power
562 balance, the total power output of G10 is forced to decrease, which means that the
563 deep cycling power of G10 is increased at the same time. This reveals that severe
564 wind power fluctuations with high spinning reserve demand during the valley load
565 periods might lead to large deep cycling power of coal units. Meanwhile, the total
566 curtailed wind power is also changed as the spinning reserve demand of the wind
567 power increases. Consequently, the increase of the spinning reserve demand of the
568 wind power is accommodated by the increase of the deep cycling power of G10 and
569 the variations of wind power curtailment.

570 **4.5 Analysis of shutting down coal units in system DB**

571 To measure the impact of the shutting down coal units, a 10 day (weekday) long

572 term generation scheduling of DB is investigated in this case, and the 1st day
573 corresponds to the case study presented in Section 4.1. Two scenarios are considered
574 in this case. In Scenario 1 (SC_1), all units in DB remain in operation. In Scenario 2
575 (SC_2), G8 whose generation capacity is the smallest (also with the shortest start-up
576 time and lowest start-up cost) in DB is attempted to be shut-down at 0:00 in the 1st
577 day. Other coal units with larger capacities are still kept in operation. Load variance is
578 smooth over the 10 days. To simplify the analysis and emphasize the comparison
579 between SC_1 and SC_2, tie line power adjustment strategy is not adopted in this
580 case.

581 Daily wind energy variance, daily deep cycling cost and wind power curtailment
582 cost of SC_1 is shown in Fig. 11.

583 According to Fig. 11, wind power also varies significantly over the 10 days. On
584 the 7th day, the wind power generation is even close to zero. Generally, deep cycling
585 costs and wind power curtailment costs have high correlation with wind energy
586 variance, which reflects that larger scale wind power may cause severer deep cycling
587 and wind power curtailment. It is also clear that wind power curtailment is adopted
588 first to avoid deep cycling of coal units. For instance, although wind power
589 curtailment exists from 2nd day to 8th day, the deep cycling cost in these days is 0.
590 However, due to the very high wind power penetration in the 9th day and 10th day,
591 deep cycling costs are very high because wind power curtailment already reaches its
592 maximum limit in these days.

593 By shutting down G8, daily deep cycling cost and wind power curtailment cost of
594 SC_2 with same wind power variance as in SC_1 is shown in Fig. 12.

595 As shown in Fig. 12, wind power curtailment costs and deep cycling costs of DB
596 are significantly reduced compared with SC_1, and deep cycling costs in these 10

597 days are all 0. However, this is based on shutting down a coal unit with an extremely
598 high start-up cost. To further analyze the economic **impact** of shutting down the coal
599 unit, total operation costs and accumulated costs indices of SC_1 and SC_2 are
600 **illustrated** in Fig. 13 and Fig. 14, respectively. In Fig. 13, the shutting down cost of
601 G8 is not included in **the** total operation costs of SC_2.

602 **Fig. 13 reveals the strong correlation of** the total operation costs of SC_1 and
603 SC_2 with the wind power variance. As G8 is kept in operation in SC_1, **the** curtailed
604 wind power and deep cycling power is very high **in day 9 and day 10 when the** wind
605 power penetration is high, causing **much higher** total operation costs of SC_1 than that
606 of SC_2. By shutting down G8, **the** total operation cost during these days can be
607 notably reduced. **Fig. 14 shows that the** C_a curve of SC_1 **increases rapidly in the** 9th
608 and 10th **days** due to the extremely high deep cycling cost and wind power curtailment
609 cost as shown in Fig 11. As C_{as} of SC_2 is higher than C_a of SC_1 in 1st day, shutting
610 down G8 is **not economic for** this day. The reason is that **a** very high start-up cost of
611 G8 greatly increases C_{as} of SC_2, incurring C_{as} of SC_2 higher than that of SC_1 in
612 **the** 1st day. From the UC **point of view**, the results in Fig. 14 show that the **impact** of
613 shutting down coal units should be reflected in a long time interval rather than day
614 scale due to the high start-up cost, which greatly distinguishes UC of WCIS from
615 other UC problems. Consequently, long **start-up** time and high **start-up** cost are both
616 **the** main reasons to fix UC of coal units day ahead in WCIS.

617 **5 Conclusions**

618 An economic dispatch strategy that makes full use of the distinctive
619 characteristics of IWCIS is proposed in this paper. Based on the distinctive operation
620 features of WCIS, the special UC characteristics of WCIS are analyzed. **Through a**
621 **proper** design of the optimization variables **for** deep cycling units in this economic

622 dispatch model of WCIS, the mixed integer optimization problem is completely
623 avoided. Case study results reveal that the model proposed in this paper can well
624 illustrate the complicated interactions between the wind power curtailment and the
625 deep cycling of coal units during valley load periods. It is shown that the impact of
626 UC of WCIS can only be reflected in a longer time interval rather than over a day
627 scale due to the extremely high start-up costs of coal units, and the wind power
628 fluctuation in the long time interval has a strong correlation with the total operation
629 cost of the system. Finally, shutting down coal units during valley load period might
630 help reduce the deep cycling and wind power curtailment of coal units. The findings
631 of this study can also be applied to interconnected systems where the RE is also a
632 WCIS. However, such systems are not common and the wind power accommodation
633 capacity of such systems is strongly restricted due to very weak EPAC of the RE.

634 **6 Acknowledgements**

635 This work is supported by EPSRC/NSFC jointly funded project ‘Intelligent Grid
636 Interfaced Vehicle Eco-charging (iGIVE)’ under Grant (Nos. EP/L001063/1 and
637 51361130153), NSFC funded project under Grant No. 61533010 and China
638 Postdoctoral Science Foundation (2013M540286).

639

640 **References**

- 641 [1] GWEC, ‘Global Wind Energy Outlook’ [Online]. Available: at
642 <http://www.gwec.net/index.php?id=181&L=pddbrgfhnvlkx>, accessed June 2010
- 643 [2] Baldick, R.: ‘Wind and energy markets: a case study of Texas’, *IEEE Syst.*
644 *Journal*, 2012, **6**, (1), pp. 27-31
- 645 [3] Aparicio, N., MacGill, I., Abbad, J., *et al.*: ‘Comparison of wind energy support
646 policy and electricity market design in Europe, the United States, and Australia’,

- 647 *IEEE Trans. Sust. Energy*, 2012, **3**, (4), pp. 809–818
- 648 [4] Bentek Energy, ‘How Less Became More Wind, Power and Unintended
649 Consequences in the Colorado Energy Market’ [Online]. Available at
650 [http://www.wind-watch.org/documents/wp-content/uploads/](http://www.wind-watch.org/documents/wp-content/uploads/BENTEK-How-Less-Became-More.pdf) BENTEK-How -Le
651 ss - Became-More.pdf
- 652 [5] Wang, C., Lu, Z., Qiao, Y.: ‘A consideration of the wind power benefits in
653 day-ahead scheduling of wind-coal intensive power systems’, *IEEE Trans.*
654 *Power Syst.*, 2013, **28**, (1), pp. 236-245
- 655 [6] Rogers, K., Ragheb, M.: ‘Symbiotic coupling of wind power and nuclear power
656 generation’. Proc. Int. Conf. 1st International Nuclear & Renewable Energy Conf.
657 (INREC), Jordan, 2010
- 658 [7] Biskas, P., Baslis, C., Simoglou, C.: ‘Coordination of day-ahead scheduling with
659 a stochastic weekly unit commitment for the efficient scheduling of slow-start
660 thermal units’. Proc. Int. Conf. Symposium - Bulk Power System Dynamics and
661 Control - VIII (IREP), Brazil, 2010
- 662 [8] U.S. Environmental Protection Agency, ‘Assessment of Startup Period at
663 Coal-Fired Electric Generating Units’ [Online]. Available at
664 <http://www.epa.gov/mats/pdfs/matsstarttsd.pdf>
- 665 [9] Simoglou, C., Biskas, P., Bakirtzis, A.: ‘Optimal self-scheduling of a thermal
666 producer in short-term electricity markets by MILP’, *IEEE Trans. Power Syst.*,
667 2010, **25**, (4), pp. 1965-1977
- 668 [10] Price, J., Rothleder, M.: ‘Recognition of extended dispatch horizons in
669 California’s energy markets’. Proc. Int. Conf. IEEE PES General Meeting,
670 Detroit, USA, 2011
- 671 [11] Southern Hami-Zhengzhou UHVDC [Online]. Available at

- 672 http://en.wikipedia.org/wiki/Southern_Hami-Zhengzhou_UHVDC
- 673 [12] Aigner, T., Jaehnert, S., Doorman, G., *et al.*: ‘The effect of large-scale wind
674 power on system balancing in Northern Europe’, *IEEE Trans. Sust. Energy*, 2012,
675 **3**, (4), pp. 751–759
- 676 [13] Khatir, A., Conejo, A., Cherkaoui, R.: ‘Multi-area unit scheduling and reserve
677 allocation under wind power uncertainty’, *IEEE Trans. Power Syst.*, 2014, **29**, (4),
678 pp. 1701-1710
- 679 [14] Yingvivatanapong, C., Lee, W., Liu, E.: ‘Multi-area power generation dispatch in
680 competitive markets’, *IEEE Trans. Power Syst.*, 2008, **23**, (1), pp. 196-203
- 681 [15] Albadi, M., Saadany, E.: ‘Overview of wind power intermittency impacts on
682 power systems’, *Electr Power Syst Res*, 2010, **80**, (6), pp. 627-632
- 683 [16] Chang, Y., Lee, T., Chen, C., *et al.*: ‘Optimal power flow of a wind-thermal
684 generation system’, *Int J Electr Power Energy Syst*, 2014, **55**, pp. 312-320
- 685 [17] Chun-Lung, C.: ‘Optimal wind-thermal generating unit commitment’, *IEEE*
686 *Trnas. Energy Convers.*, 2008, **23**, pp. 273-280
- 687 [18] Doherty, R., Outhred, H., O’Malley, M.: ‘Establishing the role that wind
688 generation may have in future generation portfolios’, *IEEE Trans. Power Syst.*,
689 2006, **21**, (3), pp. 1415-1422
- 690 [19] Chung, K., Kim, B., Hur, D.: ‘Multi-area generation scheduling algorithm with
691 regionally distributed optimal power flow using alternating direction method’,
692 *Int. J. Electr. Power Energy Syst.*, 2011, **33**, (9), pp. 1527-1535
- 693 [20] Souroudi, A., Rabiee, A.: ‘Optimal multi-area generation schedule considering
694 renewable resources mix: a real-time approach’, *IET Gener. Transm. Distrib.*,
695 2013, **7**, (9), pp. 1011–1026
- 696 [21] Abdullah, M., Muttaqi, K., Agalgaonkar, A., *et al.*: ‘New approach for sharing

- 697 wind generation spatial diversification in multi-area power systems using
698 trade-off analysis', *IET Gener. Transm. Distrib.*, 2014, **8**, (8), pp. 1466–1478
- 699 [22] U.S. Department of Energy, 'Analysis Methodology for Balancing Authority
700 Cooperation in High Penetration of Variable Generation' [Online]. Available at
701 http://www.pnl.gov/main/publications/external/technical_reports/PNNL-19229.pdf
702 f
- 703 [23] Yang, X., Song, Y., Wang, G., *et al.*: 'A comprehensive review on the
704 development of sustainable energy strategy and implementation in China', *IEEE*
705 *Trans. Sust. Energy*, 2010, **1**, (2), pp. 57–65
- 706 [24] Pinson, P.: 'Estimation of wind power forecast uncertainty' (Dissertation style),
707 2006, Ecole des Mines de Paris
- 708 [25] Wang, S., Yu, J.: 'Optimal sizing of the CAES system in a power system with
709 high wind power penetration', *Int. J. Electr. Power Energy Syst.*, 2012, **37**, pp.
710 117-125

711

712 **Figure Captions**

- 713 Fig. 1 Typical load and wind power curve of a WCIS in Northern China.
- 714 Fig. 2 Simplified topology of IWCIS.
- 715 Fig. 3 Flow chart of the adjustment of tie line power plan.
- 716 Fig. 4 Deep cycling model of coal units for generation scheduling.
- 717 Fig. 5 Geographical diagram of the studied interconnected power system.
- 718 Fig. 6 Predicted load and wind power of DB during valley load period.
- 719 Fig. 7 Deep cycling power and wind power curtailment of system DB during valley load period.
- 720 Fig. 8 Optimal tie line power adjustment.
- 721 Fig. 9 Power adjustment of deep cycling and wind farm clusters.
- 722 Fig. 10 Deep cycling power of G10 and total curtailed wind power in DB when $R_{\text{wdn},t}$ is 70 MW.

723 Fig. 11 Daily deep cycling cost and wind power curtailment cost of SC_1.

724 Fig. 12 Daily deep cycling cost and wind power curtailment cost of SC_2.

725 Fig. 13 Total operation cost of SC_1 and SC_2.

726 Fig. 14 Accumulated cost of SC_1 and SC_2.

727 **Table Captions**

728 Table 1 Generation equipment of WCIS in Northern China.

729 Table 2 Generating equipment and capacities of DB.

730 Table 3 Original day-ahead tie line plan.

731 Table 4 Parameters of coal units in system DB.

732 Table 5 Generation scheduling of the system DB during valley load period.

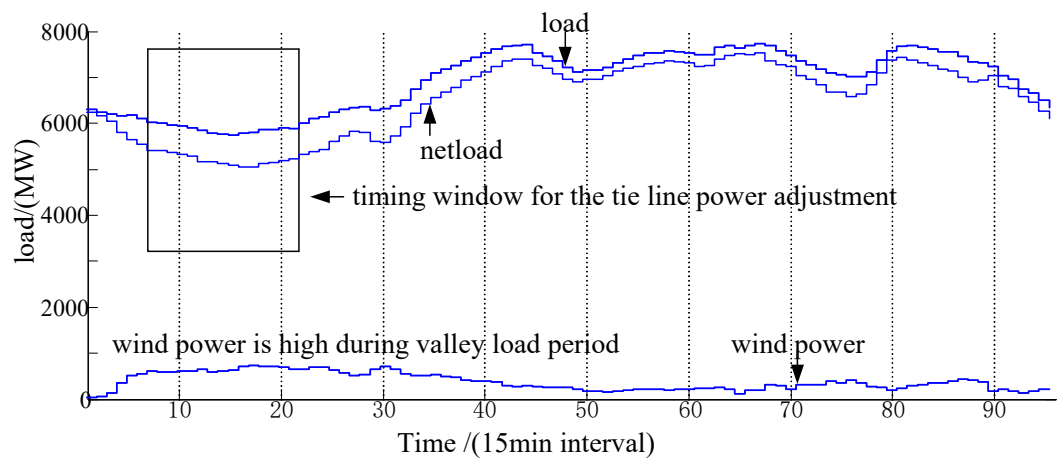


Fig. 1. Typical load and wind power curve of a WCIS in Northern China.

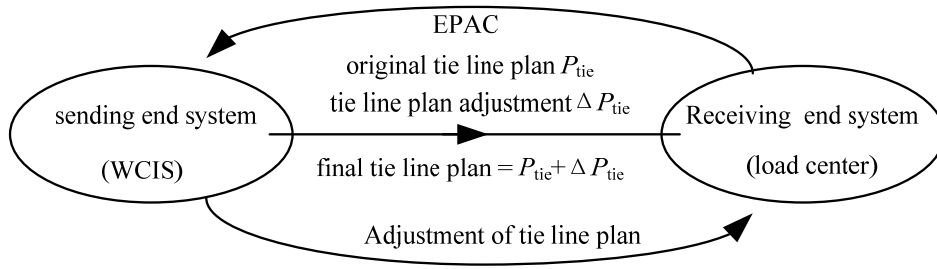


Fig. 2. Simplified topology of IWCIS.

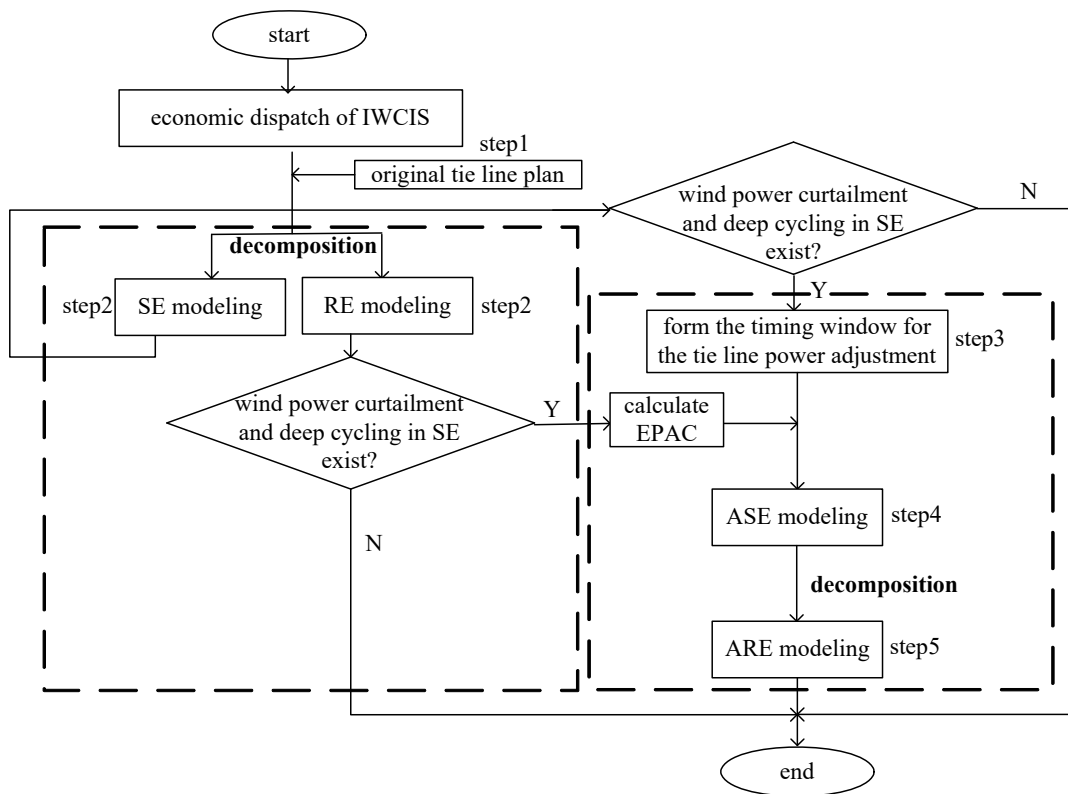


Fig. 3. Flow chart of the adjustment of tie line power plan.

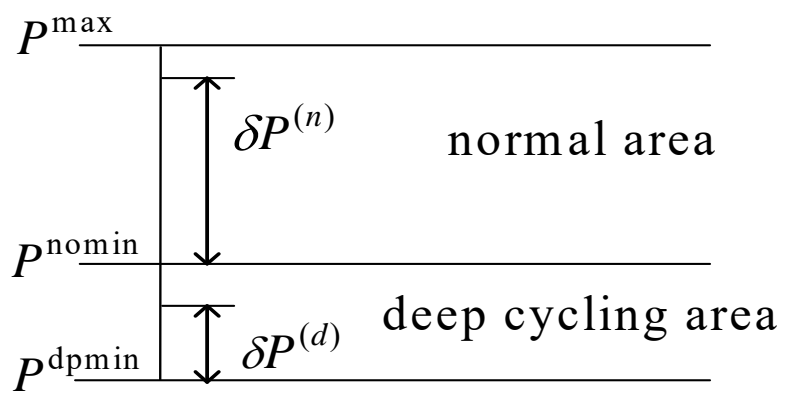


Fig. 4. Deep cycling model of coal units for generation scheduling.

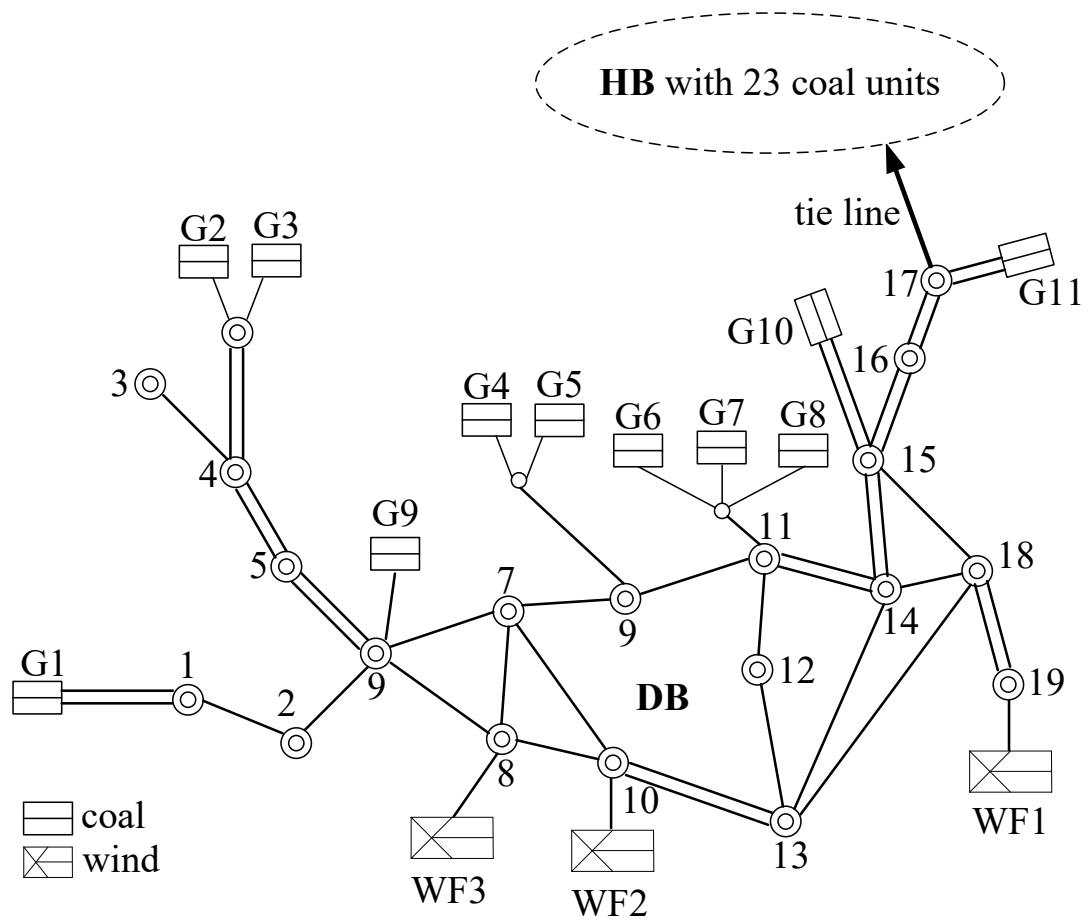


Fig. 5. Geographical diagram of the interconnected DB and HB.

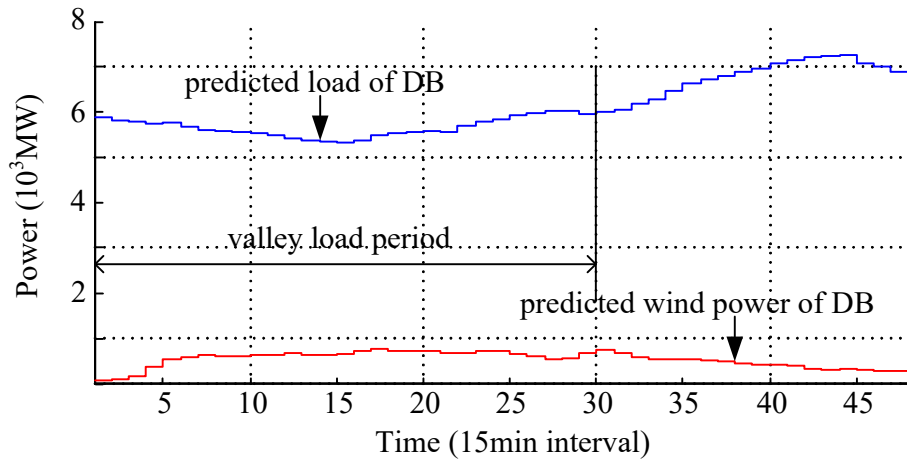


Fig. 6. Predicted load and wind power of DB during valley load period.

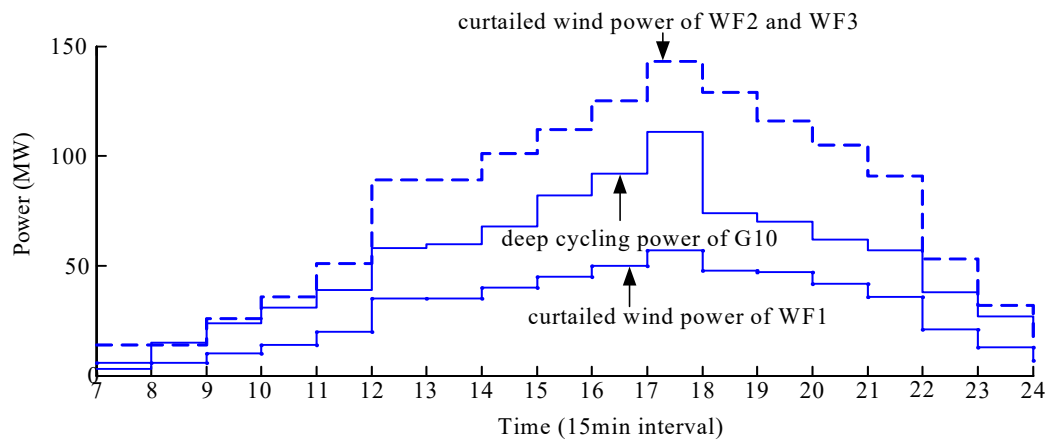


Fig. 7. Deep cycling power and wind power curtailment of system DB during valley load period.

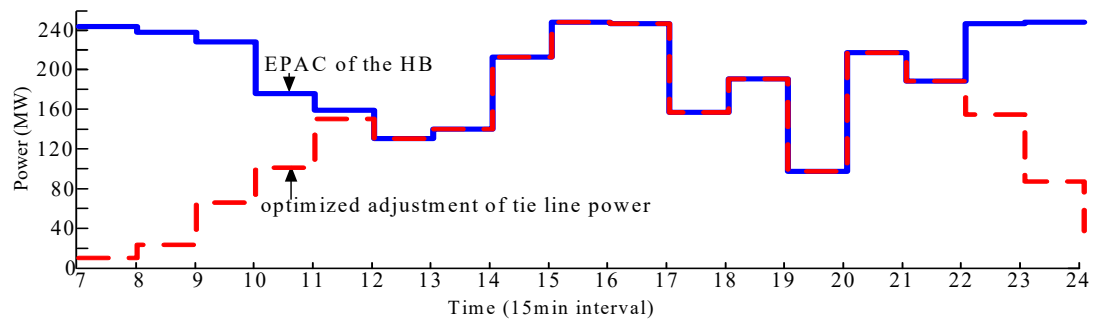


Fig. 8. Optimal tie line power adjustment.

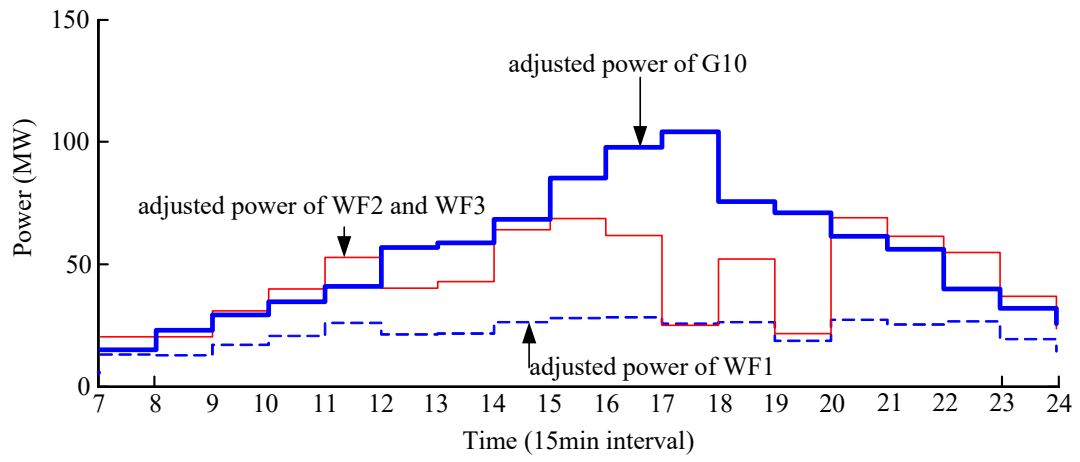


Fig. 9. Power adjustment of deep cycling and wind farm clusters.

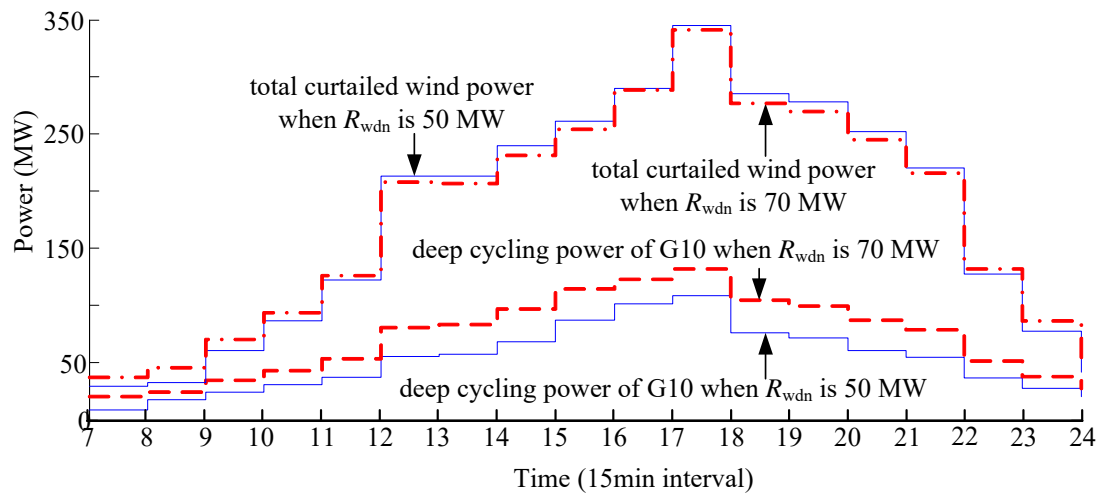


Fig. 10. Deep cycling power of G10 and total curtailed wind power in DB when $R_{wdn,t}$ is 70 MW.

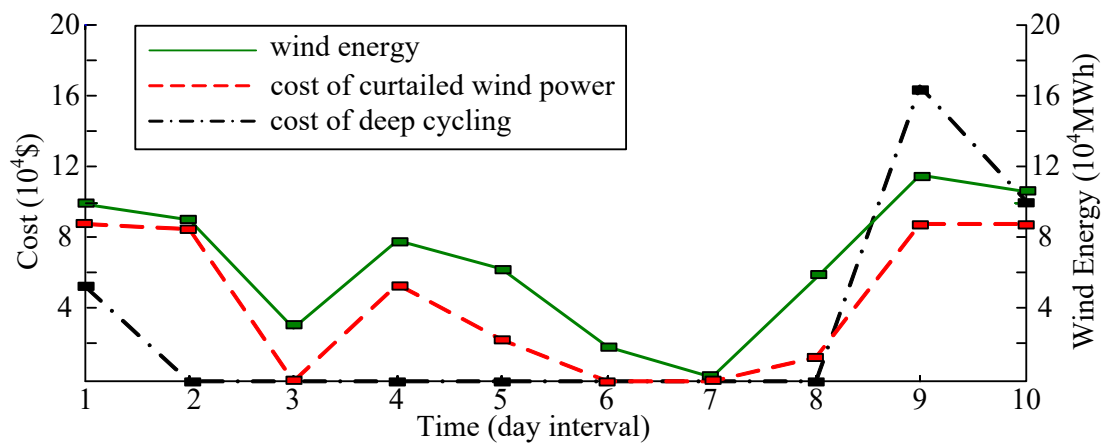


Fig. 11. Daily deep cycling cost and wind power curtailment cost of SC_1.

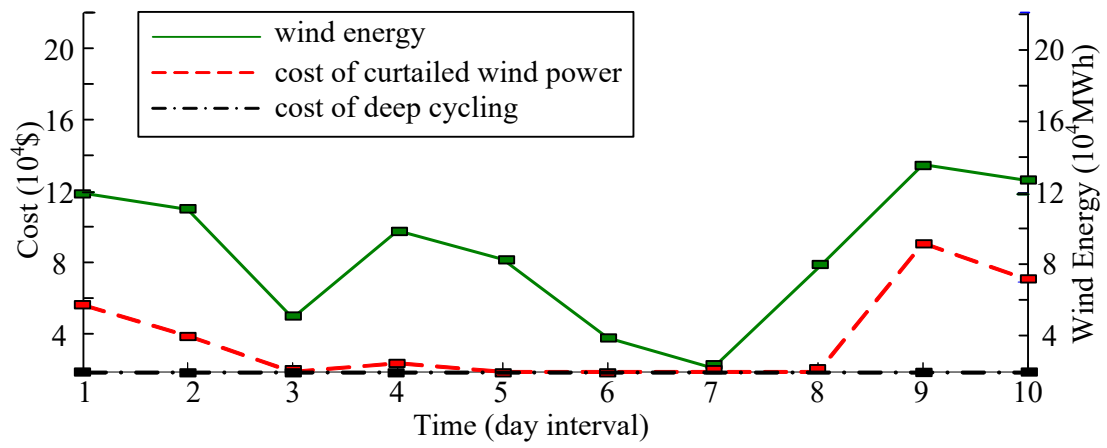


Fig. 12. Daily deep cycling cost and wind power curtailment cost of SC_2.

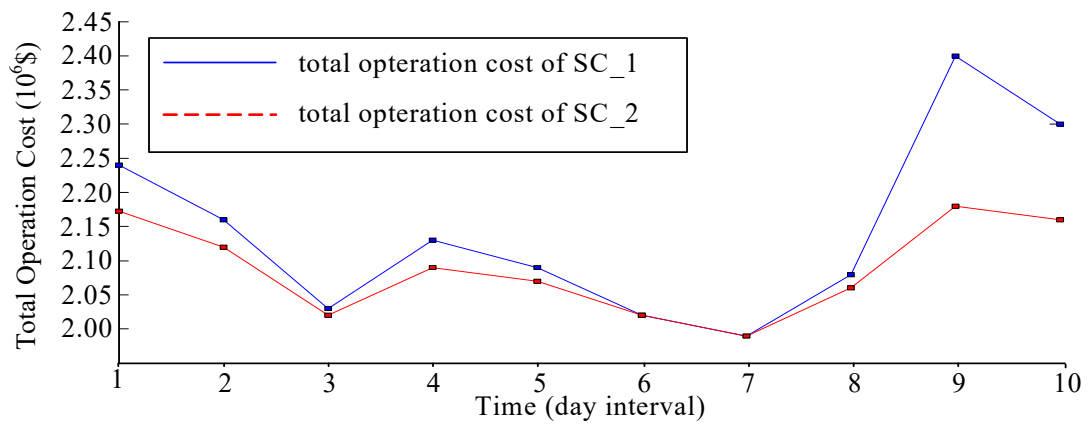


Fig. 13. Total operation cost of SC_1 and SC_2.

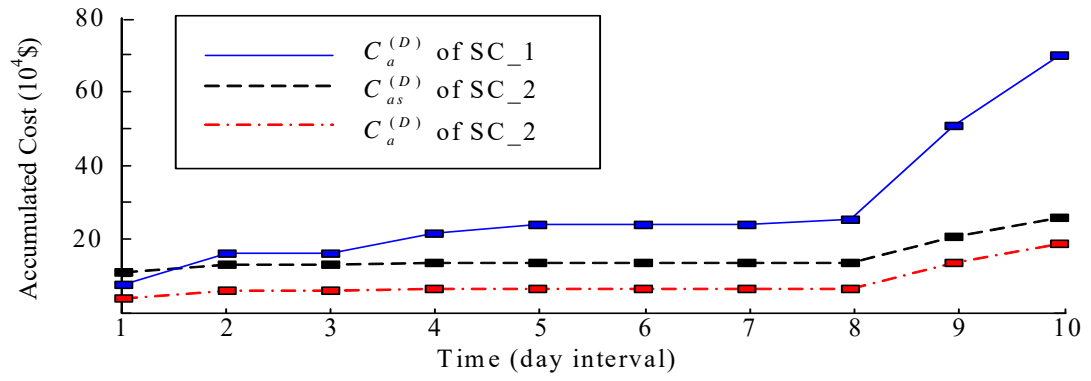


Fig. 14. Accumulated cost of SC_1 and SC_2.

Table 1
Generation equipment of WCIS in Northern China

Power output	Coal	Wind	Nuclear (planned)	Energy storage systems
Max MW	7900	1200	600	200
Min MW	5440	0	600	-150

Table 2
Generating equipment and capacities of DB

	Capacity MW	Percentage of the total capacity %
Total capacity	9100	100.0
Coal power	7900	86.8
Wind power	1200	13.2
Tie line	1500	N/A

Table 3

Original day ahead tie line plan

Time interval	Tie line plan MW	Time interval	Tie line plan MW
1-16	630	49-64	930
17-32	480	65-80	750
33-48	690	81-96	660

Table 5
Generation scheduling of the system DB during valley load period

Name	Dispatched power output MW											
	5	6	7*	8*	9*	10*	11*	12*	13*	14*	15*	16*
G1	984	975	970	970	970	970	970	970	970	970	970	970
G2, G3	243	230	220	220	220	220	220	220	220	220	220	220
G4, G5	415	406	400	400	400	400	400	400	400	400	400	400
G6-G8	243	236	230	230	230	230	230	230	230	230	230	230
G9	1026	1014	1000	1000	1000	1000	1000	1000	1000	1000	1000	1000
G10 $\delta P^{(d)}$	260	260	252	243	236	230	223	205	203	192	173	159
G10 $\delta P^{(n)}$	24	11	0	0	0	0	0	0	0	0	0	0
G11 $\delta P^{(d)}$	200	200	200	200	200	200	200	200	200	200	200	200
G11 $\delta P^{(n)}$	25	11	0	0	0	0	0	0	0	0	0	0
WF1	0	0	5	6	10	14	20	35	35	40	43	48
WF2	0	0	12	13	25	36	51	89	89	100	109	121
WF3	0	0	12	13	25	36	51	89	89	100	109	121
EPAC of HB	246	245	242	237	229	183	168	143	151	215	246	245

Name	Dispatched power output MW											
	17*	18*	19*	20*	21*	22*	23*	24*	25	26	27	28
G1	970	970	970	970	970	970	970	970	975	984	993	991
G2, G3	220	220	220	220	220	220	220	220	231	244	254	252
G4, G5	400	400	400	400	400	400	400	400	407	417	426	424
G6-G8	230	230	230	230	230	230	230	230	236	244	250	249
G9	1000	1000	1000	1000	1000	1000	1000	1000	1015	1027	1040	1037
G10 $\delta P^{(d)}$	152	184	189	200	206	224	233	240	260	260	260	260
G10 $\delta P^{(n)}$	0	0	0	0	0	0	0	0	11	26	39	36
G11 $\delta P^{(d)}$	200	200	200	200	200	200	200	200	200	200	200	200
G11 $\delta P^{(n)}$	0	0	0	0	0	0	0	0	11	26	39	36
WF1	57	47	46	42	36	21	13	7	0	0	0	0
WF2	144	119	116	105	92	53	32	17	0	0	0	0
WF3	144	119	116	105	92	53	32	17	0	0	0	0
EPAC of HB	166	196	114	219	194	245	246	246	166	196	114	219